Structure and Property Modification of Bimodal Molecular Weight Distribution Polyethylene by Electron Beam Irradiation

Sang Man Lee, Hye-Jin Jeon, Sun Woong Choi, and Hyun Hoon Song*

Department of Advanced Materials, Hannam University, Daejeon 306-791, Korea

Young Chang Nho

Radiation Application Division, Korea Atomic Energy Research Institute, Daejeon 305-600, Korea

Kyucheol Cho

S. K. Corporation, Daejeon 300-712, Korea

Abstract: Polyethylene of bimodal molecular weight distribution was irradiated with an electron beam. The thermal and mechanical properties were examined by DSC, small and wide angle X-ray scattering and static tensile test according to the crystal morphology of the irradiated samples. The crystal morphology change upon irradiation, as revealed by wide angle X-ray scattering, correlated well with the changes in melting enthalpy, whereas the lamellar thickness and the amorphous gap thickness remained virtually unchanged at irradiation doses up to 500 kGy. Crosslinks in the crystal domains became evident at an energy level of 250 kGy, resulting in reduced crystallinity and crystal size of the (110) and (200) planes. The samples became stiff and brittle with increased irradiation dose, which seem to be more relevant to the amount of crosslinks than the crystal morphology changes.

Keywords: bimodal molecular weight distribution PE, electron beam irradiation, crystal morphology, mechanical property.

Introduction

The plastic industry has shown rapid growth in the last half century and they become the most extensively utilized materials in replacement of metals and ceramics. Among variety of polymeric materials, polyolefins including polyethylene and polypropylene are the most popular commodity polymers and its application is continuously expanding. Efforts to improve their properties also have been continuously attempted. In particular, the polyethylene of bimodal molecular weight distribution (BMWD) is a new material which shows a superior mechanical and processing property over the conventional unimodal molecular weight distribution polyethylene (UMWDPE).

When the BMWDPE undergoes crystallization to form alternating crystal-amorphous layer structure, it is expected that the high molecular weight species allow abundant tie chains between the crystalline lamellar units and thus provides the stability against the long term fatigue. On the other hand, the low molecular weight specie mainly forms the

crystal lamellae, providing the stiffness of the material.[1-3] Such unique property of BMWDPE is very useful to meet the requirements of plastic pipe.

One other technique improving the polymer mechanical properties is by introducing the crosslinks in the polymer sample. Among several methods to induce crosslinks in the polymers, the high energy electron beam or gamma irradiation is the most popular ones.[4-14] They require relatively short time for the reaction to occur and the process is simple compared to the method of chemical treatment.

In this work, the BMWDPE was irradiated with the electron beam and subsequent changes in microstructures and physical properties were examined.

Experimental

Materials. The samples used in this study were high density polyethylene of bimodal molecular weight distribution, YUZEX™. The polymer was obtained from SK Corporation. The sheets of 1 mm thickness for the tests were made by the compression molding of the polymer samples. To avoid the orientation often induced by the pressure during

*Corresponding Author. E-mail: songhh@hannam.ac.kr

the compression molding, the samples were relaxed at the molding temperature (190 °C) after releasing the molding pressure.

Electron Beam Irradiation. An electron beam accelerator (model ELV-4) was used for the irradiation of our samples. The maximum irradiation energy was 1 MeV with a stability of ± 2%. The operating power was 50 kW with a maximum current of 40 mA. The irradiation doses were selected as 100, 250, 500, and 1,000 kGy. The heat generated during the irradiation was removed by the aluminum cooling plate.

Characterization. Thermal properties of the samples were examined by a differential scanning calorimeter (DSC) (TA 2910) under the nitrogen gas atmosphere. The heating and cooling was done at 10 °C/min for the samples of 4 ± 1 mg. From the results of DSC, various structural parameters including the melting temperature (T_m), crystalline temperature (T_c), heat of fusion (ΔH), and degree of crystallinity were obtained.

The tensile properties were tested using a tensile tester (Shimadzu AG-500G) at 3 mm/min and room temperature. The specimen size was $5 \times 1 \times 54$ mm based on ASTM D638.

Both small and wide angle X-ray scattering were performed for the detailed structural analysis from several nanometers to tens of nanometer scale. The small angle X-ray scattering experiment was carried out utilizing the synchrotron radiation at Pohang Accelerator Laboratory.[15,16] The wave length of X-ray beam was 1.608 Å and beam size at the sample position was 0.4×0.4 mm. Sample-to-detector distance was 1,100 mm and a 2-dimensional position sensitive area detector was used for the data collection. For the wide angle X-ray scattering, a Rigaku powder diffractometer attached to a rotating anode generator (RU 300) operated at 40 kV and 70 mA was utilized. The wavelength was 1.54 Å (Cu Kα) and the data collection was made at $2\theta=$ 12-27 degrees with a resolution of 0.01 degree.

X-Ray Data Analysis. The X-ray intensities scattered from the irradiated samples contain structural information of different length scale, depending the scattering angles where the data are collected. The analysis of wide angle X-ray scattered intensities are rather straight forward. It provides the crystal size estimation or the crystal perfection and the crystallinity. On the other hand, the analysis of scattered intensities from the small angles requires mathematical manipulation to gain some useful structural information. The raw intensity curve from the semicrystalline polymer provides the long period which represents the average distance of the crystal lamellar domains or the amorphous layer gap between the crystal lamellar stacks. In order to separate these two individual quantities from the raw SAXS intensity profiles, a correlation function analysis[17-19] need to be carried out. In an isotropic case, the correlation function, $\gamma(r)$, is given as
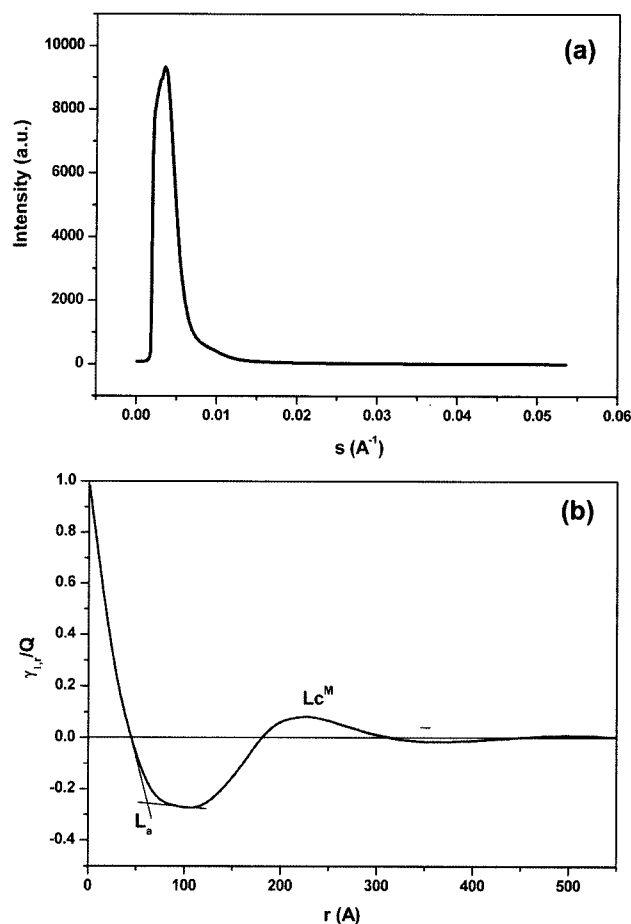

Figure 1. A typical small angle X-ray scattered pattern of lamellar structure (a) and the correlation function derived from the scattered intensities (b).

$$\gamma(r) = \frac{\int I(s) \times \cos 2\pi r s\, ds}{\int I(s) ds} \qquad (1)$$

where s is the scattering angle defined as $2\sin\theta/\lambda$ and r is the correlation length. Figure 1 depicts an example of correlation function which reveals the lamellar long spacing, lamellar thickness, and amorphous layer thickness.

Results and Discussion

Thermal Properties. DSC thermograms of irradiated samples are plotted in Figure 2. Melting point (T_m) and melting enthalpy (ΔH) derived from the DSC thermograms are also plotted in Figure 3. In general, melting enthalpy (ΔH) is associated with the amount of crystalline part, while T_m is with the thickness or the perfection of the crystal domains.[20] On the other hand, factors affecting the crystal thickness are the branch content, chemical impurities, and crystallization temperature. AS shown in the Figure 3, the
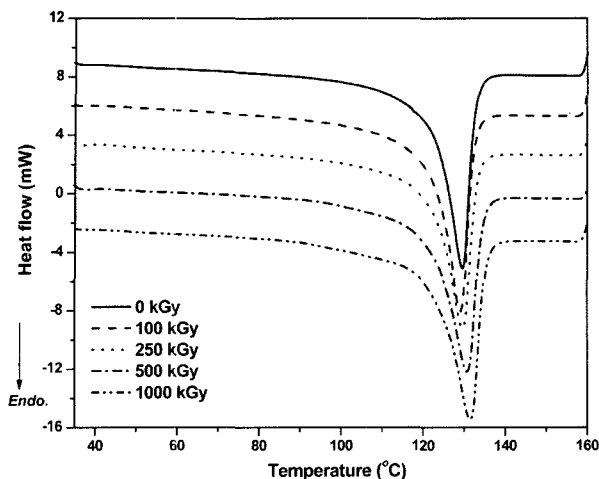
Figure 2. DSC thermograms of electron beam irradiated samples. The curves are arbitrarily shifted.
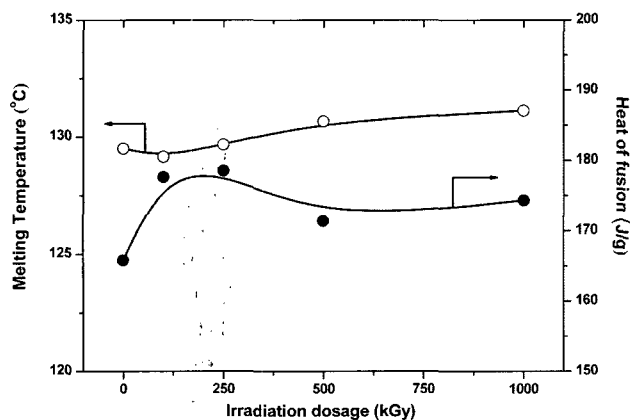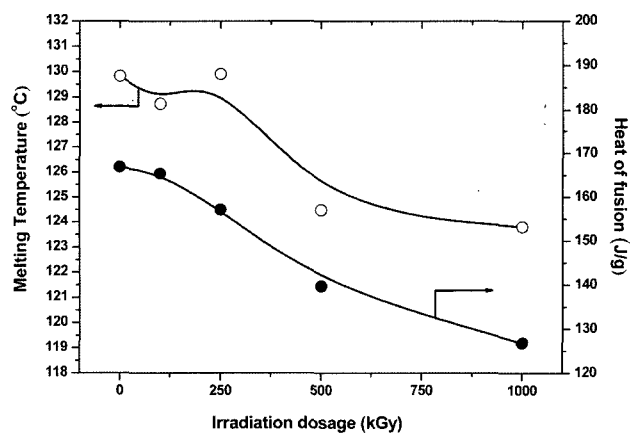

Figure 3. Melting temperature and heat of fusion of irradiated samples at different irradiation dosage.

melting point shows gradual increase with the irradiation dose and reaches the highest value at the highest dose of 1,000 kGy. The enthalpy, on the other hand, reaches a maximum near the 250 kGy and decreases on further increase of the irradiation dose. The increase of melting point upon irradiation can be attributed to either the change of crystal morphology or the crosslinks formed within the chains. The former can be related with the crystal size, especially the lamellar thickness and the crystal perfection. The latter, on the other hand, can be attributed to the reduced entropy gain in the melting of crosslinked chains in comparison to the melting of ordinary linear chains. It is also noted that the increase of melting point seems to be more marked above the irradiation dose of 250 kGy, where the melting enthalpy begins to decrease.

As discussed previously, in BMWD polymer the short low molecular weight chains are more likely to form single lamellar units in the crystallization process. On the other

hand, the high molecular weight chains will have a higher chance of forming several crystal lamellar units and the gap filling amorphous layers between them. In this case, the chains at the amorphous layers are acting as tie chains connecting the lamellar units, providing superior mechanical properties. When the electron beam is irradiated, the chain scission shall take place first in the low density amorphous region rather than in the crystalline part. The chain scission then raises the local chain mobility which allows the recrystallization or increase of the crystal perfection, thus increase of the melting points.[21-31] Here, the long chain species are more likely to be involved in this changing process. The initial increase of melting enthalpy with the irradiation dose shown in the Figure 3 confirms the crystallization induced by the chain scission. As already mentioned, the melting enthalpy begins to decrease as the irradiation dose reaches above 250 kGy, indicating the reduction of the crystallinity. The energy level at this stage is apparently sufficient enough for the electron beams to penetrate into the crystal domains and to induce structural changes within the crystal domains. The similar results showing that 250 kGy is the level where the crystal domains are effected were reported with the HDPE samples.[32] The increase of melting point even at this dosage level can be attributed to the crosslink formation within the crystal domains, yielding the reduction in entropy gain during the crystal melting.
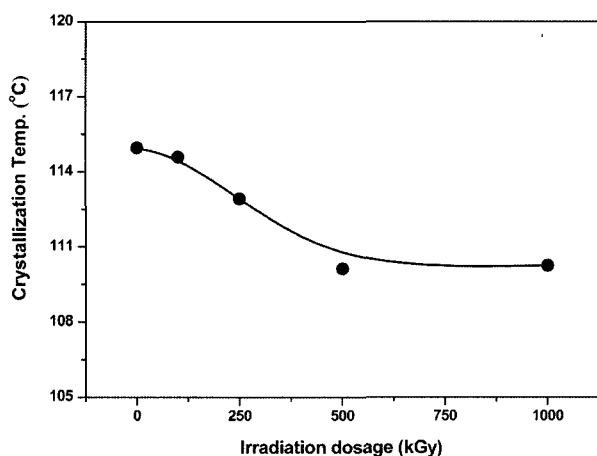
Structural changes at the molecular level induced by the high energy irradiation can also be estimated by examining the recrystallization process of the irradiated samples. The irradiated samples were heated above the melting temperature and recrystallized by the subsequent cooling process. The thermal properties of the recrystallized samples were then examined by the DSC and the results are depicted in Figure 4. The results of recrystallized sample exhibit somewhat different thermal behaviors from those of original irradiated samples. Marked reduction in melting temperatures and melting enthalpy with the irradiation doses can be noted,
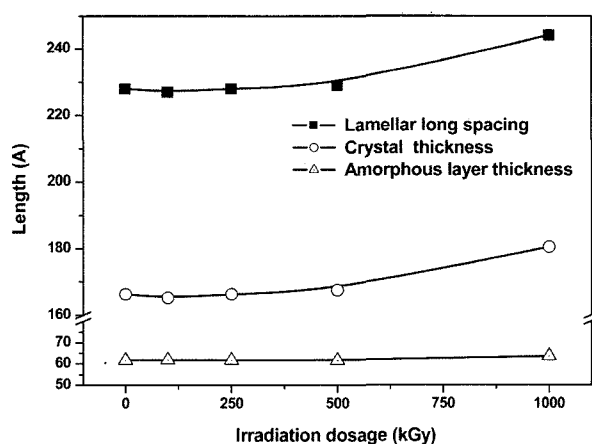

Figure 4. Melting temperature and heat of fusion of irradiated samples after recrystallization.

especially at the high level dose. The results strongly suggest the high level of crosslink formation, which is apparently not favorable for the crystal formation. Crystallization temperatures of the irradiated samples obtained during the recrystallization process upon cooling are also plotted in Figure 5. The decrease of crystallization temperature with the irradiation dose confirms the retardation of crystal growth of the crosslinked chains.

X-Ray Structures. From the small angle X-ray scattered intensities, the lamellar long spacing, individual lamellar and amorphous layer thickness were derived using the correlation function analysis.[17-19] The results are plotted in Figure 6. As depicted in the plot, the lamellar long spacing increases with the irradiation dose. The lamellar thickness and amorphous gap derived from the correlation analysis show that the increase of long spacing is mainly from the increase of the lamellar thickness. The amorphous gap between the crystal lamellae remains nearly constant over the whole

range of the irradiation dose. One very interesting observation is that the lamellar thickness increase is only minimal at the low doses, but large increase of thickness is noted between the dose level of 500 and 1,000 kGy. Recalling our results of thermal properties discussed before, the high level of crosslinks and reduction in melting enthalpies were observed at this dosage level. The results are completely different from the results of UHMWPE reported earlier,[32] where the continuous decrease of the lamellar long spacing with the irradiation was noted. In this case, the decrease of lamellar long spacing was mainly from the reduction of the amorphous layer thickness. The lamellar thickness rather increased at the low irradiation doses followed by a reduction in the thickness on further increase of irradiation. We are not certain of the origin of these discrepancies noted between the BMWDPE and UHMWPE. Nevertheless, one may speculate that the differences are associated with the molecular weight distribution of the polymers.

The correlation function analysis of the SAXS intensity data allows one to estimate the vertical dimension of the crystal lamella and its variations. On the other hand, the crystal thickness of (110) or (200) planes obtained by the Scherrer's equation provides the lateral dimension of the lamellar stacks. In Figure 7, crystal thicknesses of (110) and (200) planes derived from the Scherrer's equation are depicted. The crystal thicknesses of (110) and (200) plane increase up to 250 kGy, then show slight decrement with the increase of electron beam irradiation. Both curves are very similar to that of heat of fusion shown in Figure 3. It is very interesting to note that the crystal dimension in the transverse direction rather than the lamellar thickness correlates well with the melting enthalpies. The results are suggesting that the change found in the melting enthalpy, i.e. crystallinity, upon irradiation is associated with the crystal growth in the transverse direction of the lamellar stacks. The crystallinity indices obtained utilizing the reflection peak and the
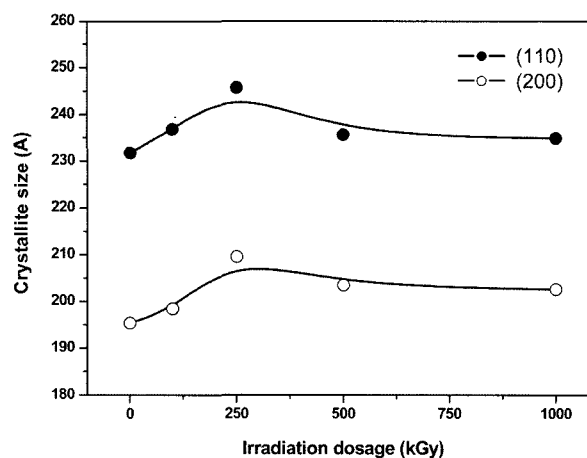

Figure 5. Crystallization temperatures of irradiated samples vs. irradiation dosage.

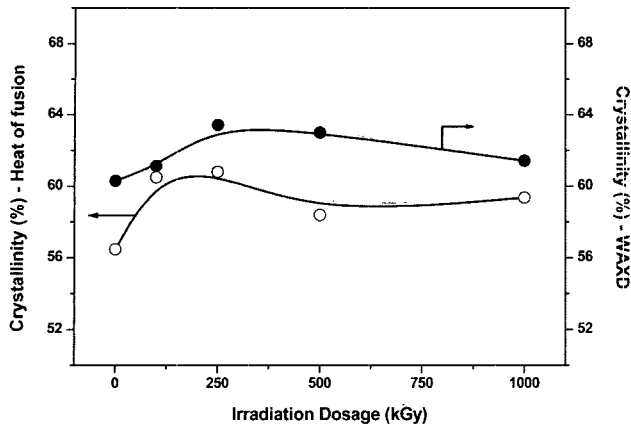
Figure 6. Changes of lamellar long period, crystal thickness and amorphous layer thickness vs. irradiation dosage.


Figure 7. Change of crystal thickness of (110) and (200) planes vs. irradiation dosage.

Figure 8. Crystallinities of irradiated samples as determined by wide angle X-ray scattering and DSC.

Figure 9. Stress-strain diagrams of irradiated samples.

melting enthalpy[33,34] are also depicted in Figure 8. They show similar trend. Initial chain scission by the irradiation induces the crystal growth, resulting in the crystal thickening in the transverse direction of lamellae. This result is consistent with the initial enhancement of melting point and melting enthalpies at the low doses. However, at the irradiation doses above the 250 kGy, the crosslinks take place between the chains within the crystal domains, yielding reduction in both crystal size and crystallinity as well as melting enthalpy.
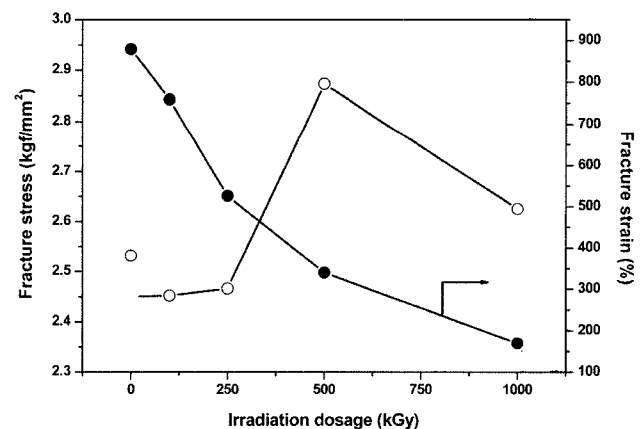
Mechanical Properties. Stress-strain curves of the irradiated samples are depicted in Figure 9. Modulus and yield stress, as well as fracture stress and strain obtained from the s-s curves are compared in Figures 10 and 11. In general, the BMWDPE shows the better mechanical properties which is associated with the enhanced crystallinity in the presence of low molecular weight species and with the tie chains of the high molecular weight ones linking between the lamellar units.[2,3,33,34] In a similar manner, chain scission and crosslinking induced by the irradiation also play a role to increase the mechanical properties even though the fracture strain decreases.[35] The crosslinks between the chains effectively prevents the slippage of the chains.[36,37] All samples show enhancement of moduli and yield stress, as shown in Figure 10, except the one of 1,000 kGy. Modulus and yield stress of polymeric materials are known to be dependent on the crystal content, crosslink density and the temperature. In our case, the crosslinks may play the main role to increase these properties. On the other hand, in samples irradiated at 1,000 kGy, the severe deterioration of polymer structure in addition to chain scission and crosslinking must have taken place, thus resulting in the reduced modulus and yield stress. However, these values are still higher than those of virgin samples. Similar effects are also noted in the fracture stress as depicted in Figure 11. The fracture strain shows monotonic decrease with the increase of irradiation dose, implying major role of crosslinks in the deforming process over the crystal morphology.
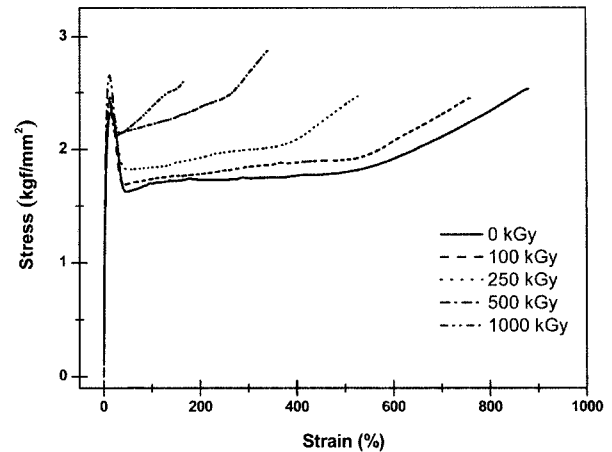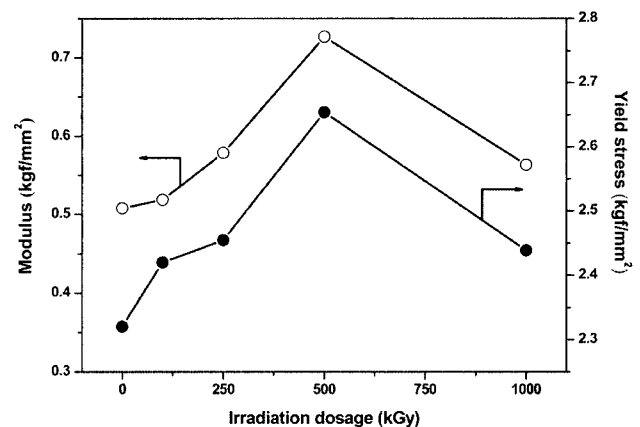
Figure 10. Changes of modulus and yield stress vs. irradiation dosage.

Figure 11. Changes of fracture strain and stress vs. irradiation dosage.

Conclusions

Polyethylene of BMWD was irradiated with the electron beam in an attempt to improve its mechanical properties. The applied dosage level of electron beam varied from 100 to 1000 kGy. When the high energy electron beam is bombarded in the polymer chains, both chain scission and cross links take place simultaneously. The early increase of crystallinity was observed from the results of X-ray scattering and DSC, which can be attributed to the temporal increase of chain mobility by the chain scission, mainly in the amorphous region. The additional crystallization reduced at 250 kGy and the crystallinity and crystal size increase diminished when the dose level reached above 250 kGy. The results implied that the energy level of 250 kGy is sufficient enough to induce chain scission and crosslink in the crystal domains. The crystalline lamellar thickness and the amorphous gap between them remained nearly constant until the dosage level reaches 500 kGy. However, the lateral dimension of the lamellar stacks, i.e. (200) or (110) crystal plane thickness, increased up to 250 kGy and decreased on further increase of the dosage. Improved mechanical properties of modulus, yield stress and polymer chains were also observed except the one of 1,000 kGy where severe structural deterioration must have occurred in addition to the chain scission and cross linking. The degree of crosslinks appeared to be more effective on the deformation process than the crystal morphology.

References

(1) M. Fleissner, *Polym. Eng. Sci.*, **38**, 330 (1998).

(2) A. Lustiger and R. L. Markham, *Polymer*, **24**, 1647 (1983).

(3) L. L. Böhm, H. F. Enderle, and M. Fleissner, *Adv. Mater.*, **4**, 234 (1992).

(4) L. Woo and C. L. Standford, *Radiat. Phys. Chem.*, **63**, 845 (2002).

(5) Y. Ikada, K. Nakamura, S. Ogata, K. Makino, K. Tajima, E. Endoh, T. Hayashi, S. Fujita, A. Fujisawa, S. Mastlda, and H. Oonisili, *J. Polym. Sci., Polym. Chem.*, **37**, 159 (1999).

(6) W. L. Sauer, K. D. Weaver, and N. B. Beals, *Biomaterials*, **17**, 1929 (1996).

(7) V. L. Auslender, A. A. Bryazgin, B. L. Faktorovich, V. A. Gorbunov, E. N. Kokin, M. V. Korobeinokov, G. S. Krainov, A. N. Lukin, S. A. Maximov, V. E. nekhaev, A. D. Panfilov, V. N. Radchenko, V. O. Tkachenko, A. A. Tuvik, and L. A. Voronin, *Radiat. Phys. Chem.*, **63**, 613 (2002).

(8) K. Nakamura, S. Ogata, and Y. Ikada, *Biomaterials*, **19**, 2341 (1998).

(9) K. Mehta, P. Fuochi, M. Lavalle, and A. Kovacs, *Radiat. Phys. Chem.*, **62**, 745 (2002).

(10) M. Takehisa, T. Saito, T. Takahashi, T. Sato, and T. Sato, *Radiat. Phys. Chem.*, **41**, 495 (1993).

(11) J. H. Kim, H. N. Cho, S. H. Kim, and J. Y. Kim, *Macromol. Res.*, **12**, 53 (2004).

(12) S. Y. Nam, Y. C. Nho, and S. H. Hong, *Macromol. Res.*, **12**, 219 (2004).

(13) L. Pruitt and R. Ranganatann, *Mat. Sci. Eng. C-Bio. S*, **3**, 91 (1995).

(14) V. Premnath, A. Bellare, E. W. Merrill, M. Jasty, and W. H. Harris, *Polymer*, **40**, 2215 (1999).

(15) J. Bolze, J. Kim, J.-Y. Huang, S. Rah, H. S. Youn, B. Lee, T. J. Shin, and M. Ree, *Macromol. Res.*, **10**, 2 (2002).

(16) M. Ree and I. S. Ko, *Phys. High Tech.(Korea)*, **14**, 2 (2005).

(17) R. J. Roe, *Methods of X-ray and Neutron Scattering in Polymer Science*, Oxford Univ. Press, New York, 2000.

(18) W. Ruland, *Colloid Polym. Sci.*, **255**, 417 (1977).

(19) W.-T. Chuang, U.-S. Jeng, H.-S. Sheu, and P.-D. Hong, *Macromol. Res.*, **14**, 45 (2006).

(20) U. W. Gedde, *Polymer Physics*, Chapman & Hall, London, 1995.

(21) G. Lewis, *Biomaterials*, **22**, 371 (2001).

(22) M. Dole, *Radiation Chemistry of Macromolecules*, Academic Press, New York, 1972.

(23) N. M. Stark and L. M. Matuana, *Polym. Degrad. Stabil.*, **86**, 1 (2004).

(24) M. Goldman, R. Gribsky, G. G. Long, and L. Pruitt, *Polym. Degrad. Stabil.*, **62**, 97 (1998).

(25) G. Lewis, *Biomaterials*, **22**, 371 (2001).

(26) V. Premnath, A. Bellare, E. W. Merrill, M. Jasty, and W. H. Harris, *Polymer*, **40**, 2215 (1999).

(27) P. H. Kang and Y. C. Nho, *Radiat. Phys. Chem.*, **60**, 79 (2001).

(28) A. Rivation, D. Lalande, and J. -L. Gardette, *Nucl. Instrum. Meth. B*, **222**, 187 (2004).

(29) A. Valenza, S. Piccaroli, and G. Spadaro, *Polymer*, **40**, 835 (1999).

(30) Q. Yu and S. Zhu, *Polymer*, **40**, 2961 (1999).

(31) K. Nishida, T. Konishi, T. Kanaya, and K. Kaji, *Polymer*, **45**, 1433 (2004).

(32) S. M. Lee, S. W. Choi, Y. C. Nho, and H. H. Song, *J. Polym. Sci., Polym. Phys.*, **43**, 3019 (2005).

(33) Y. Q. Wang and J. Li, *Mater. Sci. Eng. A-Struct.*, **266**, 155 (1999).

(34) T. Ozawa, *Polymer*, **12**, 150 (1971).

(35) J. Scheirs, L. L. Böhm, J. C. Boot, and P. S. Leevers, *TRIP*, **4**, 408 (1996).

(36) P. H. Kang, J. S. Park, and Y. C. Nho, *Macromol. Res.*, **10**, 332 (2002).

(37) N. G. McCrum, C. P. Buckley, and C. B. Bucknall, *Principles of Polymer Engineering*, Oxford Science Publications, New York, 1997.